Coherent Terahertz Polarization Control through Manipulation of Electron Trajectories

Haidan Wen[1] and Aaron M. Lindenberg[1,2]

[1]PULSE Institute, SLAC National Accelerator Laboratory, Menlo Park, California, 94025, USA
[2]Department of Materials Science and Engineering, Stanford University, Stanford, California, 94305, USA

(Received 3 March 2009; published 7 July 2009; publisher error corrected 1 September 2009)

The dynamics of ionized electrons in a plasma can be controlled by synthetic optical fields composed of the fundamental and the second harmonic of femtosecond optical pulses with an arbitrary phase and polarization. We show here that the plasma-emitted half-cycle THz radiation directly reflects the two-dimensional trajectories of the electrons through polarization sensitive THz emission spectroscopy. As a result, we find that the THz polarization smoothly rotates through 2π radians as the relative phase between the two pulses is adjusted, providing a new means of coherently controlling the polarization of light at THz frequencies.

DOI: 10.1103/PhysRevLett.103.023902 PACS numbers: 42.65.Re, 52.38.−r

In order to access ultrafast radiation whose spectrum is out of the reach of conventional lasing media, methods are needed for manipulating and controlling the electron dynamics associated with nonlinear light-matter interactions on ultrafast time scales. In the gas phase, laser-produced plasmas represent low-cost nonlinear media with high damage thresholds in which electrons can be ionized and manipulated by synthetic optical fields on time scales of an optical cycle, leading to emission across a broad spectrum from x-ray to THz frequencies. Depending on the birth time during the optical cycle, ionized electrons oscillating in the laser field can either recollide with parent ions to radiate extreme ultraviolet pulses through the high harmonic generation process [1,2], or can drift away generating a time-dependent current and radiating electromagnetic field pulses at THz frequencies [3–5]. The emission spectrum and intensity can be tuned through control of the optical waveform via either the carrier envelope phase of a few-cycle pulse [6,7] or the relative phase of a two-color field [8,9]. Similar one-dimensional processes in solid-state samples have also been observed [10–12]. In this Letter, we demonstrate the control of electron trajectories in two spatial dimensions by a synthesized optical field composed of the fundamental and the second harmonic. As a result, the polarization of the radiated near-half-cycle THz field can be continuously rotated through 2π radians as the relative phase is adjusted. We thus show that THz emission spectroscopy enables visualization of the complex electron trajectories in a plasma in real time, providing new understanding of the plasma-based THz generation mechanism. All-optical control of the electron trajectories enables ultrafast manipulation of the polarization state with application to imaging [13,14], dichroism [15], and polarimetry [16,17] at THz frequencies.

Whereas THz generation in a laser-produced plasma pumped by a two-color field has been widely used as a source for nonlinear THz spectroscopy [18–20], further optimization of the source has been inhibited by a lack of understanding of the generation process. Recently, this has been interpreted microscopically as the radiation from a one-dimensional transient current [3,4] or through a four-wave mixing process mediated by the plasma [9,21], both of which predict that the THz emission is completely suppressed at certain relative phases (at 0 and $\pi/2$, respectively). The relative phase has thus been used as an important criterion to validate these models experimentally [3]. We show here that the THz field amplitude does not vanish at certain relative phases in general if the fundamental and second harmonic fields are not parallel. Instead, the polarization undergoes a continuous rotation as a function of the relative phase. Utilizing both THz emission spectroscopy and theoretical simulations, we demonstrate that this can be understood as a result of the development of a transient current in the transverse plane whose direction is controlled by the relative phase of the two-color field.

A superposition of the fundamental and the second harmonic optical fields is created by focusing a 50 fs, 0.8 mJ, 800 nm laser pulse through a 100 μm type-I beta-barium borate (BBO) crystal (Fig. 1). At the focus, the estimated fundamental and second harmonic optical intensity is about 6.0×10^{14} W/cm^2 and 3.5×10^{13} W/cm^2, respectively, generating a plasma with estimated electron density 3×10^{16} cm^{-3}. The superposed fields tunnel-ionize the air and drive a time-dependent current, leading to THz emission in the forward direction. The THz field is selected by a thick Teflon filter from the residual optical beams and collected by a pair of off-axis parabolic mirrors. A rotatable wire-grid THz polarizer (contrast $>$ 95:1 below 3 THz) is used to characterize the THz polarization before either a liquid-helium-cooled InSb hot-electron bolometer or an electro-optical (EO) sampling setup [22]. To vary the relative phase of the fundamental and the second harmonic field, the crystal-to-plasma distance is adjusted. The relative phase change $\Delta\varphi$ is related to the change of the BBO position Δd by $\Delta\varphi = \omega(n_\omega - n_{2\omega})\Delta d/c$, where c is the speed of light in vacuum and n_ω and $n_{2\omega}$ are the refractive indices of the air. The relative polarization of the optical beams can be independently controlled by rotating

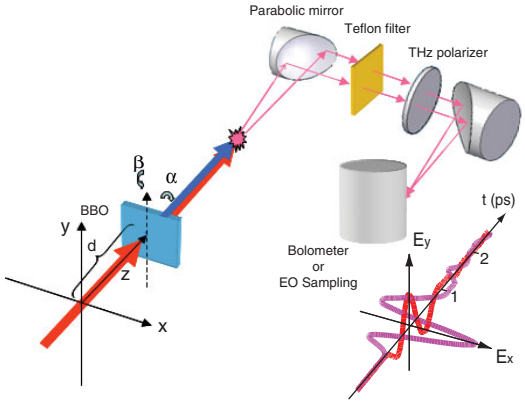

FIG. 1 (color online). The experimental setup: An 800 nm beam is focused through a BBO crystal to create a plasma that radiates THz fields. Also shown are THz waveforms measured by electro-optical sampling with BBO position at $d = 0$ mm (purple or light gray) and $d = 13$ mm (red or gray), corresponding to $\pi/2$ relative phase difference, with half-cycle THz field polarization close to E_x and E_y respectively.

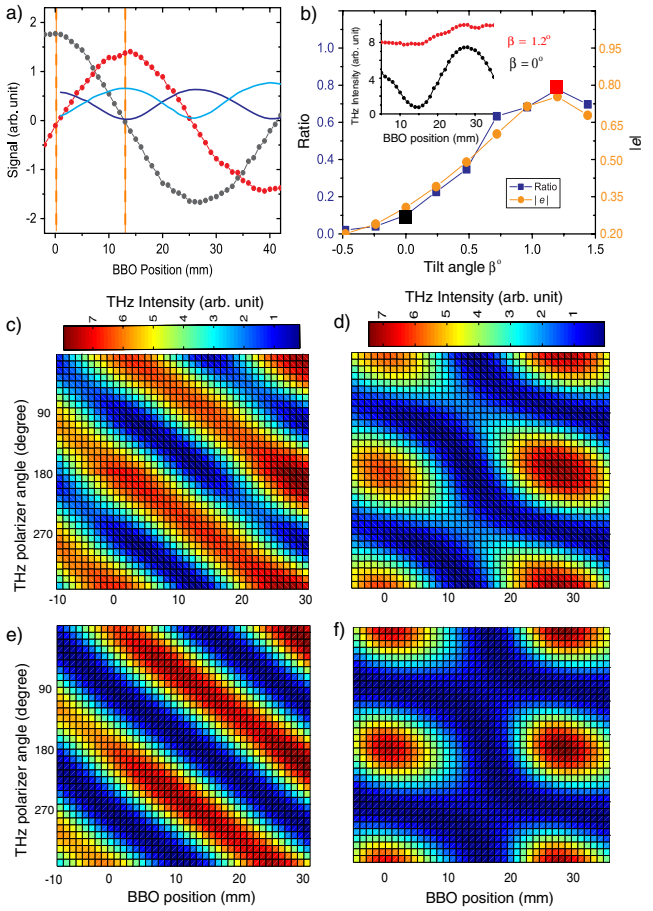

FIG. 2 (color online). (a) The transmitted THz intensity through a horizontally (solid blue or dark gray) or vertically (solid cyan or gray) oriented THz polarizer as a function of the BBO crystal position, indicating polarization rotation of the THz field when the relative phase changes by $\pi/2$. Also shown are corresponding electro-optic sampling measurements (dots, see text). (b) The ratio (blue or dark gray) of minimum to maximum THz intensities during 2π radian change of the relative phase as a function of the BBO tilt angle, β. The measured ellipticity (orange or light gray) of the 800 nm pulse shows a similar dependence on β. (inset) THz intensity as a function of relative phase for two different tilt angles. (c),(d) Transmitted THz intensity as a function of the BBO position and the THz polarizer angle at tilt angles $\beta = 1.2°$ and $\beta = 0°$, respectively. (e), (f) The simulation of (c),(d), considering the change of the second harmonic doubling efficiency when translating the BBO crystal.

the BBO crystal, with maximum THz generation occurring when the extraordinary axis of the BBO crystal is oriented at $\alpha = 55°$ with respect to the polarization of the fundamental beam along the **x** axis. By recording the transmitted THz intensity through polarizers while varying the BBO crystal position [Fig. 2(a), solid lines], we identify that a horizontally polarized THz field becomes vertically polarized with comparable intensity when the BBO crystal is moved from 0 to 13 mm as marked by the dashed line, corresponding to a $\pi/2$ relative phase change. Because the EO sampling signal is inherently sensitive to both polarization and amplitude, the measured EO signal falls from maximum to zero when the THz field rotates 90° with constant amplitude [black circle, Fig. 2(a)], in agreement with the prediction of Ref. [23]. If the ZnTe crystal orientation is reoptimized in the EO setup, the rotated THz field again yields a strong EO signal [red or gray circle, Fig. 2(a)], confirming the existence of an orthogonally polarized THz field. We note that THz polarization control and detection have also been demonstrated by microstructuring of photoconductive antennas [15,24].

To capture the full dependence of the THz polarization on the relative phase, we bolometrically record the THz transmission through the THz polarizer while changing the polarizer angle and the BBO crystal position [Figs. 2(c) and 2(d)]. The shift in the maximum THz transmission as a function of the BBO position indicates that the THz polarization continuously rotates as the relative phase changes. It is observed that when the incident beam is normal to the BBO crystal ($\beta = 0$, Fig. 1), the emitted THz field amplitude changes as well [Fig. 2(d)], varying between 36 and 10 kV/cm, with minimum THz field perpendicular to the maximum THz field. Surprisingly, the modulation of the THz amplitude for different THz polarizations can be minimized by slight rotation of the BBO crystal ($\Delta\beta =$ 1.2°) along the **y** axis, giving rise to a continuous rotation of the THz field with constant field amplitude [Fig. 2(c)]. To characterize the angular dependence of the THz generation, we record the total THz intensity without the THz polarizer as a function of the BBO crystal position at various BBO tilt angles (β). Two representative scans [inset, Fig. 2(b)] show that the intensity modulation varies dramatically with tilt. It is found the ratio of the minimum to maximum THz intensities over 2π change of the relative phase is correlated with the variation in the 800 nm beam ellipticity as the birefringent crystal is tilted [Fig. 2(b)].

In order to understand the observed polarization control of the THz field, we consider a two-color pump field that is composed of the fundamental and second harmonic pulses with arbitrary relative phase and polarization. The optical field at time t can be written as

$$\mathbf{E}(t)_L = E_\omega(t)(\cos(\omega t + \Gamma)\cos\alpha\hat{\mathbf{x}}' + \cos(\omega t)\sin\alpha\hat{\mathbf{y}}') + E_{2\omega}(t)\cos(2\omega t + \varphi)(\cos\alpha\hat{\mathbf{x}} + \sin\alpha\hat{\mathbf{y}}), \quad (1)$$

where $\hat{\mathbf{x}}'$ and $\hat{\mathbf{y}}'$ are the unit vectors of the extraordinary and ordinary axes of the BBO crystal and the 800 nm laser field has initial polarization along $\mathbf{x}$ axis. The carrier phase of the optical light is not explicitly shown. Γ represents the phase retardation between $\hat{\mathbf{x}}'$ and $\hat{\mathbf{y}}'$ polarized 800 nm laser fields that is acquired during the propagation in the birefringent BBO crystal and $E_\omega(t) = A_\omega e^{-4\ln 2(t/\tau_\omega)^2}$ is the envelop function with amplitude A_ω and pulse duration τ_ω. In prior work, the field projection on the $\mathbf{x}$ axis has been considered as the driving field for the THz generation process [21,25] while the $\hat{\mathbf{y}}$ component has been neglected. However, it is the $\hat{\mathbf{y}}$ component that liberates the ionized electrons drifting along the $\mathbf{x}$ axis to other directions in the transverse plane. Figures 3(a) and 3(b) show resulting optical synthetic fields at different relative phases of the optical fields. The electron density $N(t)$ is estimated using the static tunneling ionization rate [7,26] $w(t) = 4\omega_a(\frac{U_{N_2}}{U_H})^{5/2}\frac{E_a}{E_L(t)}\exp(-\frac{2E_a}{3E_L(t)}(\frac{U_{N_2}}{U_H})^{3/2})$ where $\omega_a = 4.134 \times 10^{16}$ s^{-1}, E_a and E_L are the atomic field and laser field, U_{N_2} and U_H are ionization potentials of hydrogen atoms and nitrogen molecules. The velocity $\mathbf{v}(t, t')$ of electrons born at t' is obtained by solving the classical equations of motion. The net time-dependent current is

$$\mathbf{J}(t) \propto \int_{-\infty}^{t} \dot{N}(t')\mathbf{v}(t, t')dt', \quad (2)$$

which sums over all possible electron birth times. The radiated THz field is then proportional to the rate of change of $\mathbf{J}(t)$, which is associated with the electron scattering process after the laser pulse. It is the direction of the net electron current that determines the polarization of the emitted THz field. The direction and amplitude of the electron current is calculated and plotted in Figs. 3(c) and 3(d) to illustrate the polarization dependence on the relative phase. The corresponding simulation [Figs. 2(e) and 2(f)] is in good agreement with the experimental observations. In the calculation of Figs. 3(c) and 3(d) we consider the ellipticity of 800 nm pump pulse during the propagation through the BBO crystal [27], yielding nonzero Γ in Eq. (1). The measured ellipticity is highly correlated with the ratio of minimum to maximum THz fields during 2π radian change of the relative phase [Fig. 2(b)]. Tilting the BBO crystal also affects other properties of the optical beam, including the reduction of the 400 nm intensity and the shift of its spectrum due to phase mismatching. But the controlled simulations suggest that they are not the dominate factors for the observed β dependence.

We further confirm this model by studying the dependence of the THz generation on the relative polarization of

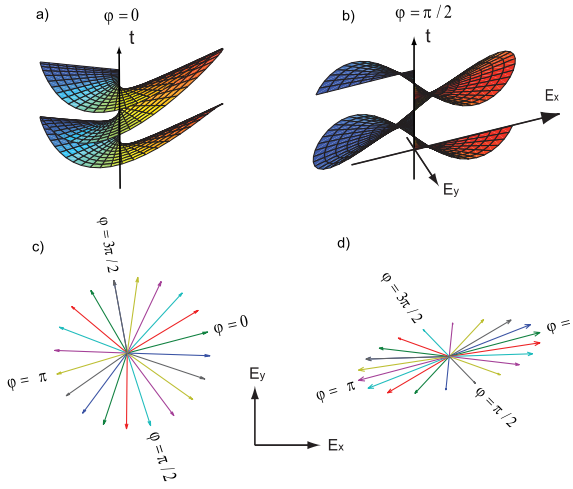

FIG. 3 (color online). (a) and (b) are the wave fronts of the two-color field at relative phase $\varphi = 0$ and $\varphi = \pi/2$, respectively, with 55° relative polarization with $\Gamma = 0$. The color shows the carrier phase of the fundamental optical field. (c) and (d) show the calculated THz polarization dependence on the relative phase for $\beta = 1.2°$ and $\beta = 0$, respectively.

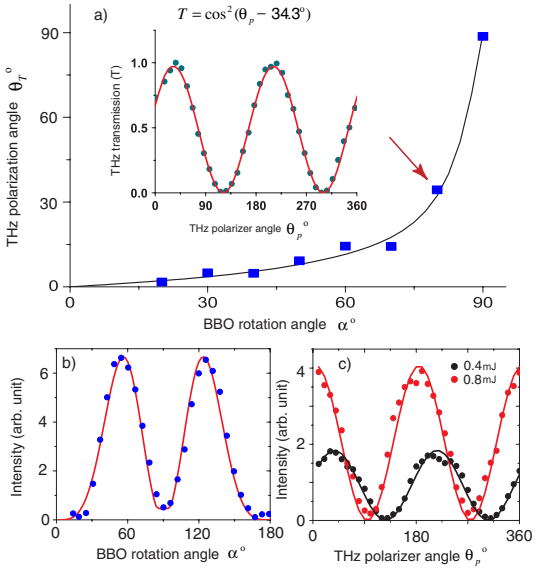

FIG. 4 (color online). (a) The THz polarization angle (squares) with respect to the fundamental optical polarization as a function of the BBO crystal rotation angle α. The solid line is calculated based on the 2-d photocurrent model. The inset shows the THz transmission (dots) as a function of the THz polarizer angle θ_p at $\alpha = 80°$ with the sinusoidal fit (solid line). (b) The total THz intensity (dots) as a function of BBO rotation angle α. The solid line represents the calculation. (c) The transmitted THz intensity (dots) through a polarizer as a function of the polarizer angle at various pump energies with sinusoidal fits (solid lines). The measurements and calculations in Fig. 4 are obtained at $d = 0$ mm and $\beta = 0$.

the optical beams and the optical pump pulse energy. The THz polarization angle θ_T with respect to the horizontal is determined by fitting the THz transmission T as a function of the polarizer rotation angle θ_p to $T = \cos^2(\theta_p - \theta_T)$ [Fig. 4(a), inset]. Its dependence on the BBO crystal angle α [Fig. 4(a)] is in good agreement with the 2-d photocurrent model described above. We also measure the total THz yield as a function of α [Fig. 4(b)]. Including the fact that the second harmonic generation efficiency also varies, the THz yield calculated by Eq. (2) agrees with the measurements well. In addition, the THz polarization is found to be dependent on the pump energy [Fig. 4(c)]. This can be explained by the phase slippage between the fundamental and second harmonic beams due to their different refractive indices in the plasma. Doubling the pump energy from 0.4 to 0.8 mJ leads to a THz polarization rotation of 32°, in good agreement with the relative phase change 39° calculated after propagation of the optical pulse through a 7 mm homogeneous plasma.

The temporal structure of the THz field (Fig. 1) measured by the EO sampling technique is not affected when changing these control parameters. As expected, the THz radiation starts from the creation of an electron current and terminates at the time when electrons scatter and lose their directional coherence. Therefore, changing the details of the synthetic field only alters the electron response during the optical pulse (50 fs) while the longer time dynamics that is responsible for the THz wave form is unaffected and determined by the scattering process. For higher pump fields or shorter pulse durations, the scattering time decreases due to the increase of the plasma density. Thus, the emitted THz pulse is shortened and its spectrum extends to higher frequency as observed in Refs. [4,28]. We note that we do not directly measure these higher frequency components through either EO sampling or bolometric measurements but expect the polarization dependence to be similar as it arises from the same generation process.

In conclusion, we have achieved all-optical coherent control of the polarization state of ultrafast THz pulses by manipulating the motion of electrons. A simple two-dimensional model of the electron trajectories explains the observed THz polarization dependence. This work provides a new understanding of the THz generation process driven by two-color fields and shows that THz emission spectroscopy is a powerful and simple tool for probing plasma electron dynamics in both space and time, in contrast to typical one-dimensional electron detector used in the coherent control experiments [29,30]. Using individually controlled optical fields [9], the THz polarization state may be switched on ultrafast time scales due to the extreme sensitivity of the polarization to the relative phase of the two optical fields. Novel applications associated with THz dichroism studies, imaging, tomography, and molecular alignment may benefit from this work.

[1] P. Corkum, Phys. Rev. Lett. **71**, 1994 (1993).
[2] M. Protopapas, C. H. Keitel, and P. L. Knight, Rep. Prog. Phys. **60**, 389 (1997).
[3] K. Y. Kim, J. H. Glownia, A. J. Taylor, and G. Rodriguez, Opt. Express **15**, 4577 (2007).
[4] K. Y. Kim, A. J. Taylor, J. H. Glownia, and G. Rodriguez, Nat. Photon. **2**, 605 (2008).
[5] M. D. Thomson, M. Kreß, T. Löffler, and H. G. Roskos, Laser Photon. Rev. **1**, 349 (2007).
[6] M. Nisoli, G. Sansone, S. Stagira, S. D. Silvestri, C. Vozzi, M. Pascolini, L. Poletto, P. Villoresi, and G. Tondello, Phys. Rev. Lett. **91**, 213905 (2003).
[7] M. Kreß *et al.*, Nature Phys. **2**, 327 (2006).
[8] N. Dudovich, O. Smirnova, J. Levesque, Y. Mairesse, M. Y. Ivanov, D. M. Villeneuve, and P. B. Corkum, Nature Phys. **2**, 781 (2006).
[9] X. Xie, J. Dai, and X.-C. Zhang, Phys. Rev. Lett. **96**, 075005 (2006).
[10] E. Dupont, P. B. Corkum, H. C. Liu, M. Buchanan, and Z. R. Wasilewski, Phys. Rev. Lett. **74**, 3596 (1995).
[11] A. Haché, Y. Kostoulas, R. Atanasov, J. L. P. Hughes, J. E. Sipe, and H. M. van Driel, Phys. Rev. Lett. **78**, 306 (1997).
[12] J. Güdde, M. Rohleder, T. Mejer, S. W. Koch, and U. Höfer, Science **318**, 1287 (2007).
[13] N. C. J. van der valk, W. A. M. van der Marel, and P. C. M. Planken, Opt. Lett. **30**, 2802 (2005).
[14] W. L. Chan, J. Deibel, and D. M. Mittleman, Rep. Prog. Phys. **70**, 1325 (2007).
[15] E. Castro-Camus, J. Lloyd-Hughes, and M. B. Johnston, Appl. Phys. Lett. **86**, 254102 (2005).
[16] N. Kanda, K. Konishi, and M. Kuwata-Gonokami, Opt. Express **15**, 11 117 (2007).
[17] H. Wen, S. N. Pisharody, J. M. Murray, and P. H. Bucksbaum, Phys. Rev. A **73**, 052504 (2006).
[18] P. Gaal, K. Reimann, M. Woerner, T. Elsaesser, R. Hey, and K. H. Ploog, Phys. Rev. Lett. **96**, 187402 (2006).
[19] P. Gaal, W. Kuehn, K. Reimann, M. Woerner, T. Elsaesser, and R. Hey, Nature (London) **450**, 1210 (2007).
[20] H. Wen, M. Wiczer, and A. M. Lindenberg, Phys. Rev. B **78**, 125203 (2008).
[21] D. J. Cook and R. M. Hochstrasser, Opt. Lett. **25**, 1210 (2000).
[22] Q. Wu and X. C. Zhang, Appl. Phys. Lett. **67**, 3523 (1995).
[23] P. C. M. Planken, H. K. Nienhuys, H. J. Bakker, and T. Wenckehach, J. Opt. Soc. Am. B **18**, 313 (2001).
[24] S. Winnerl, B. Zimmermann, F. Peter, H. Schneider, and M. Helm, Opt. Express **17**, 1571 (2009).
[25] M. Kress, T. Löffler, S. Eden, M. Thomson, and H. G. Roskos, Opt. Lett. **29**, 1120 (2004).
[26] L. D. Landau and E. M. Lifshitz, *Quantum Mechanics* (Pergamon, New York, 1965).
[27] X. C. Zhang (private communication).
[28] T. Bartel, P. Gaal, K. Reimann, M. Woerner, and T. Elsaesser, Opt. Lett. **30**, 2805 (2005).
[29] D. W. Schumacher and P. H. Bucksbaum, Phys. Rev. A **54**, 4271 (1996).
[30] H. Ohmura and M. Tachiya, Phys. Rev. A **77**, 023408 (2008).